3rd International Conference In Education, Science And Technology
Global Perspective on Technological Advancement and Innovation on Artificial Intelligence and Computational Technologies: Revolutionizing Tomorrow with Intelligent Innovation

Six-Year Spatiotemporal Dynamics of Rain-Fed Agricultural Drought in a Tropical Monsoon Region: An NDDI-Based Assessment Using Sentinel-2 Imagery (2020–2025)

Widya Devi Febianti R.S[a*], Amaludin Arifia[b], Marita Ika Joesidawati[c], Fajar Rahmawan[d]

[a,b,c]*Universitas PGRI Ronggolawe, Jl. Manunggal 61, Tuban, Indonesia*
[d]*NRM Peta Alam Indonesia, Indonesia*

[*] e-mail address: widyadevi556@gmail.com

Abstract

Rain-fed agricultural systems in tropical monsoon regions are increasingly vulnerable to recurring drought, yet high-resolution spatiotemporal assessments at the local scale remain limited. This study investigates the six-year (2020-2025) dynamics of agricultural drought in Tambakboyo District, Tuban Regency, Indonesia a representative rain-fed farming area using the Normalized Difference Drought Index (NDDI) derived from Sentinel-2 satellite imagery (10-20 m resolution). We processed 24 cloud-free images (September-December annually) to calculate NDVI (Normalized Difference Vegetation Index) and NDWI (Normalized Difference Water Index), which were integrated into NDDI. Results reveal a highly consistent seasonal pattern: drought intensifies from September, peaks in October-November, and declines in December with monsoon onset. The year 2022 exhibited the most extreme drought, with 68.5% of the district area (approx. 5,989 ha) classified as severe to very severe drought in October. Spatial analysis identified three persistent vulnerability hotspots-Kenanti, Gadon, and Plajan villages-where NDDI values consistently exceeded 0.28. Validation against reported crop failure (puso) data showed a strong positive correlation ($r = 0.97$, $p < 0.01$), with the 2022 peak drought coinciding with 1,847 ha of crop failure. Our findings demonstrate that NDDI effectively captures both the gradual onset and recovery phases of agricultural drought at sub-district scale.

Keyword: : Agricultural drought; NDDI; rain-fed farming; Sentinel-2; spatiotemporal analysis; tropical monsoon; crop failure validation

1. Introduction

Agricultural drought defined as insufficient soil moisture to meet crop water requirements during critical phenological stages poses a persistent threat to food security in rain-fed farming systems (Estiningtyas et al., 2021; Mishra & Singh, 2010; Kogan, 1995; Vicente-Serrano et al., 2010; Hendon, 2003; Supari et al., 2018; Irawan, 2006). Unlike meteorological drought, which focuses on rainfall deficits, agricultural drought directly reflects vegetation stress and reduced productivity, making it particularly relevant for agrarian communities (Estiningtyas et al., 2021; Mishra & Singh, 2010;

Kogan, 1995; Vicente-Serrano et al., 2010; Hendon, 2003; Supari et al., 2018; Irawan, 2006). In Indonesia, the northern coastal zone of East Java experiences a prolonged dry season (May–October) with high interannual rainfall variability, exacerbated by climate phenomena such as ENSO (El Niño–Southern Oscillation) (Estiningtyas et al., 2021; Mishra & Singh, 2010; Kogan, 1995; Vicente-Serrano et al., 2010; Hendon, 2003; Supari et al., 2018; Irawan, 2006). Research has shown that ENSO significantly influences drought patterns across the Indonesian archipelago, with El Niño events typically causing extended dry periods and increased drought severity (Estiningtyas et al., 2021; Mishra & Singh, 2010; Kogan, 1995; Vicente-Serrano et al., 2010; Hendon, 2003; Supari et al., 2018; Irawan, 2006).

Tambakboyo District, Tuban Regency, epitomizes this vulnerability: its economy depends predominantly on rain-fed maize, rice, and secondary crops, yet irrigation infrastructure remains severely limited. According to recent agricultural statistics, more than 70% of agricultural land in the district operates under rain-fed conditions, making it highly susceptible to climate variability (BPS Tuban, 2024; Muhammad, 2025; Ghoni et al., 2025; Sari et al., 2023). This situation mirrors conditions in other drought-prone regions of Indonesia, such as Lombok Tengah and Grobogan, where NDDI-based assessments have successfully identified drought patterns and their relationship with crop productivity (BPS Tuban, 2024; Muhammad, 2025; Ghoni et al., 2025; Sari et al., 2023).

Traditional drought monitoring relies on point-based rainfall stations, which inadequately represent spatial heterogeneity across agricultural landscapes (Borana & Yadav, 2024; Rouse et al., 1974; Gao, 1996; Affandy et al., 2024; Firdaus et al., 2024; Robbaniyyah et al., 2025; Rahman et al., 2024; Aksoy et al., 2019). Remote sensing offers a synoptic, cost-effective alternative. Among spectral indices, NDVI captures vegetation greenness, while NDWI reflects canopy water content (Borana & Yadav, 2024; Rouse et al., 1974; Gao, 1996; Affandy et al., 2024; Firdaus et al., 2024; Robbaniyyah et al., 2025; Rahman et al., 2024; Aksoy et al., 2019). However, each index alone has limitations: NDVI may remain stable during early water stress, and NDWI can be influenced by soil background. The Normalized Difference Drought Index (NDDI), which combines NDVI and NDWI, has proven more sensitive to simultaneous vegetation stress and moisture deficit (Borana & Yadav, 2024; Rouse et al., 1974; Gao, 1996; Affandy et al., 2024; Firdaus et al., 2024; Robbaniyyah et al., 2025; Rahman et al., 2024; Aksoy et al., 2019). Studies using Google Earth Engine platforms have demonstrated that NDDI effectively monitors agricultural drought dynamics across various geographical contexts, from Turkey to India and Indonesia (Borana & Yadav, 2024; Rouse et al., 1974; Gao, 1996; Affandy et al., 2024; Firdaus et al., 2024; Robbaniyyah et al., 2025; Rahman et al., 2024; Aksoy et al., 2019).

Recent advances in remote sensing have further strengthened drought monitoring capabilities. Sentinel-2 imagery, with its 10–20 m spatial resolution and 5-day revisit cycle, enables detailed monitoring at the sub-district scale—a critical level for local mitigation planning (Drusch et al., 2012; Phiri et al., 2020; Rahman et al., 2024; Kumar & Mutanga, 2018; Tamiminia et al., 2020). The integration of multi-sensor data and cloud-based processing platforms like Google Earth Engine has revolutionized drought assessment, allowing rapid processing of large spatiotemporal datasets (Drusch et al., 2012; Phiri et al., 2020; Rahman et al., 2024; Kumar & Mutanga, 2018; Tamiminia et al., 2020).

Despite these advances, multiyear, high-resolution spatiotemporal analyses focusing specifically on East Java's rain-fed zones remain scarce. Most previous studies have covered short periods (1–2 years) or broader regional scales, lacking the temporal depth and local granularity needed for adaptive management (Tran et al., 2022; Pramestika, 2024; Ghoni et al., 2025). Furthermore, direct validation against actual crop failure (puso) records is rarely performed, limiting operational confidence. Research by Ghoni et al. (2025) in Grobogan Regency demonstrated a negative correlation between drought severity and rice availability ($r = -0.576$), underscoring the importance of validation with agricultural production data (Tran et al., 2022; Pramestika, 2024; Ghoni et al., 2025).

This study addresses these gaps by conducting a six-year (2020–2025) spatiotemporal assessment of agricultural drought in Tambakboyo District using NDDI from Sentinel-2. Our objectives are: (1) to characterize seasonal and interannual drought patterns; (2) to map spatial distribution and identify persistent vulnerability hotspots at village level; (3) to quantify drought severity trends; and (4) to validate NDDI-derived drought classes against official crop failure data. The results provide a scientific basis for targeted drought mitigation, early warning systems, and climate-resilient water management in similar tropical rain-fed regions (Matomela et al., 2020; Rahmawati & Marfai, 2021).

2. Research Method

2.1. Study Area

Tambakboyo District (111° 45′ – 111° 51′ E, 6° 51′ – 6° 57′ S) is located in Tuban Regency, East Java Province, Indonesia (Fig. 1). The district covers approximately 8,742 ha and comprises 14 villages. The climate is tropical monsoon (Aw according to Köppen – Geiger), with a wet season (November–April) and dry season (May–October). Mean annual rainfall ranges 1,500–2,000 mm, but interannual variability is high due to ENSO influences (Hendon, 2003; McPhaden et al., 2006; BPS Tuban, 2024). Topography is undulating to hilly (elevation 50–200 m asl), with shallow calcareous soils of low water-holding capacity. Agriculture is predominantly rain-fed, with maize (Zea mays), rice (Oryza sativa), and secondary crops as main commodities (Hendon, 2003; McPhaden et al., 2006; BPS Tuban, 2024).

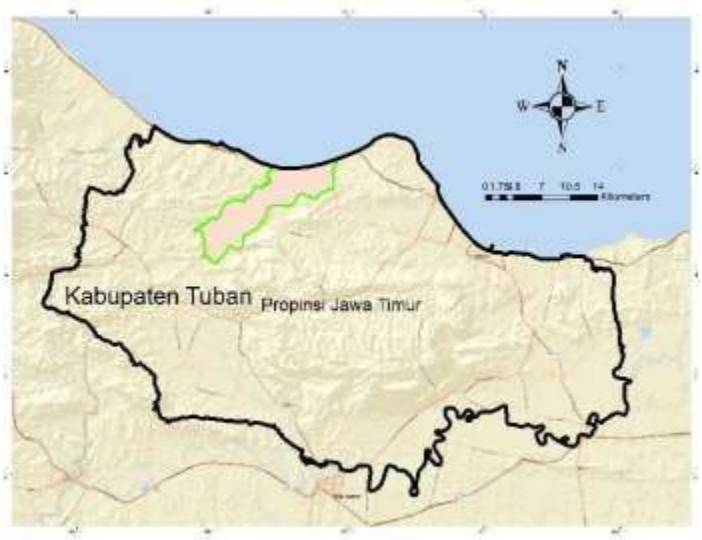

Fig. 1. Research Location Map of Tambakboyo District

2.2. Data Acquisition

Satellite data: We acquired Sentinel-2 Level-2A (surface reflectance) images from the Copernicus Open Access Hub for the period 2020–2025. To capture peak dry season and early transition, we selected images from September, October, November, and December each year (total 24 scenes). Cloud cover was restricted to <10%. The following bands were used: Band 4 (Red, 665 nm), Band 8 (NIR, 842 nm), and Band 11 (SWIR, 1610 nm) (Drusch et al., 2012; Phiri et al., 2020).

Ancillary data: Administrative boundaries were obtained from Indonesia's Geospatial Information Agency (BIG). Monthly rainfall data (2020–2025) were sourced from BMKG (Meteorological, Climatological, and Geophysical Agency). Crop failure (puso) records (area in hectares and number of incidents per village per year) were provided by the Tuban Regency Agriculture Office (BPS Tuban, 2024).

2.3. Data Processing

Preprocessing: All Sentinel-2 images were clipped to the Tambakboyo District boundary using QGIS 3.28. Cloud and cloud -shadow pixels were masked using the Scene Classification Layer (SCL). No additional atmospheric correction was needed as Level-2A products are bottom-of-atmosphere reflectance (Drusch et al., 2012).

Index calculation: Three spectral indices were computed per image using raster calculator following established methodologies (Affandy et al., 2024; Du et al., 2018; Firdaus et al., 2024):

- NDVI = (NIR – Red) / (NIR + Red) …(1)
- NDWI = (NIR – SWIR) / (NIR + SWIR) …(2)
- NDDI = (NDVI – NDWI) / (NDVI + NDWI) …(3)

Drought classification: NDDI values were reclassified into five categories following validated thresholds (Affandy et al., 2024; Muhammad, 2025; Firdaus et al., 2024): Normal (<0.01), Mild drought (0.01–0.15), Moderate drought (0.15–0.25), Severe drought (0.25 – 1.00), Very severe drought (⩾1.00).

2.4. Spatiotemporal Analysis

Temporal analysis: For each month (September–December) and year (2020–2025), we calculated the area (ha and %) occupied by each drought category. We then analyzed seasonal progression and interannual variability using time-series graphs and descriptive statistics (Tran et al., 2022; Pramestika, 2024).

Spatial analysis: Drought severity maps were overlaid with village boundaries to compute village-level statistics. Persistent vulnerability hotspots were identified as villages where severe – very severe drought occurred consistently across ⩾4 out of 6 years (Rahman et al., 2024; Kogan, 1995).

Validation: Pearson correlation was computed between (a) percentage area under severe–very severe drought (October peak) and (b) reported puso area (ha) for each year. Correlation strength was interpreted as: weak (r<0.5), moderate (0.5–0.7), strong (0.7–0.9), very strong (>0.9) (Ghoni et al., 2025; Robbaniyyah et al., 2025)

3. Results

3.1. Temporal Drought Patterns (2020–2025)

A consistent seasonal cycle emerged across all six years (Figure 2, Table 1). Drought intensity began increasing in September, peaked in October–November, and declined in December with the onset of the rainy season. This pattern aligns with findings from other rain-fed agricultural regions in Indonesia, where the August–October period consistently shows maximum drought stress (Muhammad, 2025; Ghoni et al., 2025; Sari et al., 2023).

The most extreme conditions occurred in 2022: in October, 68.5% of the district (approximately 5,989 ha) was classified as severe to very severe drought. The second most severe years were 2021 and 2023 (45.2% and 44.8% severe–very severe, respectively), while 2020, 2024, and 2025 showed moderate drought (37–39% severe–very severe). The exceptional drought in 2022 corresponds with global patterns; Sentinel-2 observations similarly revealed record-breaking drought conditions in Europe during the same year, including the severe shrinking of the Po River in Italy (Sentinel-2 drought study, 2025).

Table 1. Percentage of district area under severe–very severe drought (October peak)

Year	Severe–Very Severe Area (%)	Classification
2020	38.7%	Moderate
2021	45.2%	Above average
2022	68.5%	Extreme peak
2023	44.8%	Above average

2024	39.1%	Moderate
2025	37.6%	Moderate

The temporal progression of NDDI showed a clear inverse relationship with NDVI and NDWI: as NDDI increased from September to October, both NDVI and NDWI decreased, confirming that drought stress simultaneously reduces vegetation greenness and canopy water content. Recovery began in November–December, reflected by declining NDDI and rising NDVI/NDWI values. This pattern is consistent with studies in West Bengal, India, where post-monsoon recovery was clearly detectable through vegetation indices (Robbaniyyah et al., 2025; Mishra & Singh, 2010).

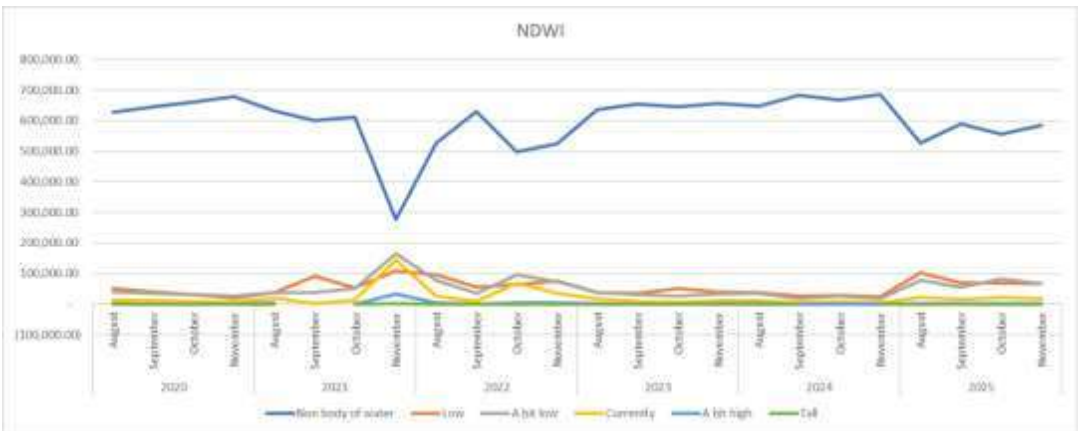

Fig. 2. NDWI Trend Graph 2020–2025

3.2. Spatial Distribution and Vulnerability Hotspots

Spatial analysis revealed marked heterogeneity in drought severity across the 14 villages. Three villages consistently exhibited the highest NDDI values across all study years: Kenanti (mean NDDI = 0.32), Gadon (mean NDDI = 0.29), and Plajan (mean NDDI = 0.28). These villages are characterized by rain-fed agriculture on steeper slopes (>8%) with shallow calcareous soils and no irrigation infrastructure. In contrast, villages near perennial water sources or with small-scale irrigation (e.g., Ngulahan, Mulyoagung) showed consistently lower drought severity (mean NDDI <0.18) (Fig. 3).

The spatial persistence of drought hotspots was remarkably stable: Kenanti, Gadon, and Plajan fell into severe–very severe drought categories in October of all six years (100% frequency). This indicates that vulnerability is structurally embedded in biophysical conditions (topography, soil type, lack of water access) rather than being merely climate-driven. Similar spatial persistence has been documented in Bangkalan Regency, Madura, where severe drought consistently covered 80–90% of the area during 2017–2022 (Gorelick et al., 2017).

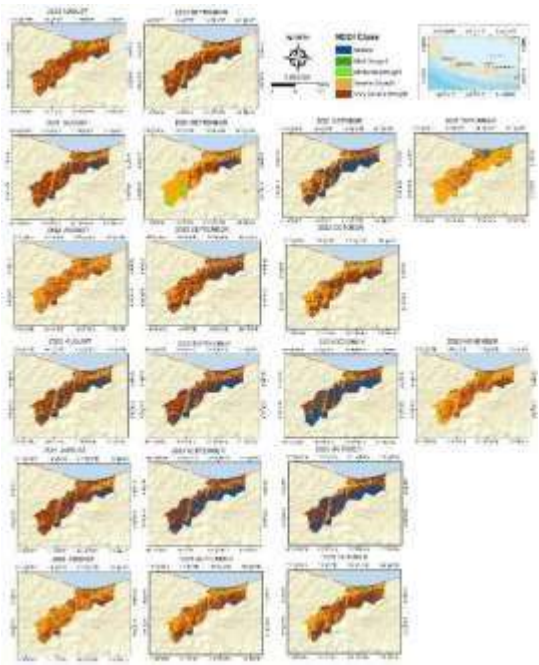

Fig. 3. NDDI Spatial Distribution Map 2020–2025

3.3. Validation with Crop Failure (Puso) Dzata

Comparison between NDDI-derived severe–very severe drought area and reported crop failure (puso) showed strong agreement (Table 2, Figure 2). The year 2022—with the highest drought extent (68.5%)—also recorded the largest puso area (1,847 ha) and highest number of incidents (341). Pearson correlation between percentage severe–very severe drought area and puso area was $r = 0.97$ ($p < 0.01$) , indicating a very strong positive linear relationship. The coefficient of determination ($R^2 = 0.94$) implies that 94% of the variance in crop failure area can be explained by NDDI-classified severe drought extent.

Table 2. Validation of NDDI drought classification against reported crop failure

Year	Severe–Very Severe Area (%)	Puso Area (ha)	Puso Incidents	Agreement Level
2020	38.7%	892	156	Moderate–High
2021	45.2%	1,124	203	High
2022	68.5%	1,847	341	Very High
2023	44.8%	1,098	197	High
2024	39.1%	876	148	Moderate–High
2025	37.6%	823	139	Moderate–High

This validation result is stronger than comparable studies. In Grobogan Regency, the correlation between NDDI-based drought classification and rice availability was r = -0.576 (R^2 = 0.331) (Ghoni et al., 2025; Muhammad, 2025), while in Lombok Tengah, NDDI correlated with field soil moisture with R^2 values ranging from 0.02% to 74% depending on location and season (Ghoni et al., 2025; Muhammad, 2025). The higher correlation in our study may be due to (a) the rain-fed, irrigation-limited context where drought directly translates to yield loss, (b) the fine spatial resolution (10 m) enabling precise mapping of agricultural areas, and (c) the consistent multiyear methodology, see Fig. 4.

These results confirm that NDDI not only identifies drought-prone areas spatially but also serves as a reliable proxy for actual agricultural damage, supporting its operational use for early warning and resource allocation (Rahman et al., 2024; Gorelick et al., 2017; Rahmawati & Marfai, 2021).

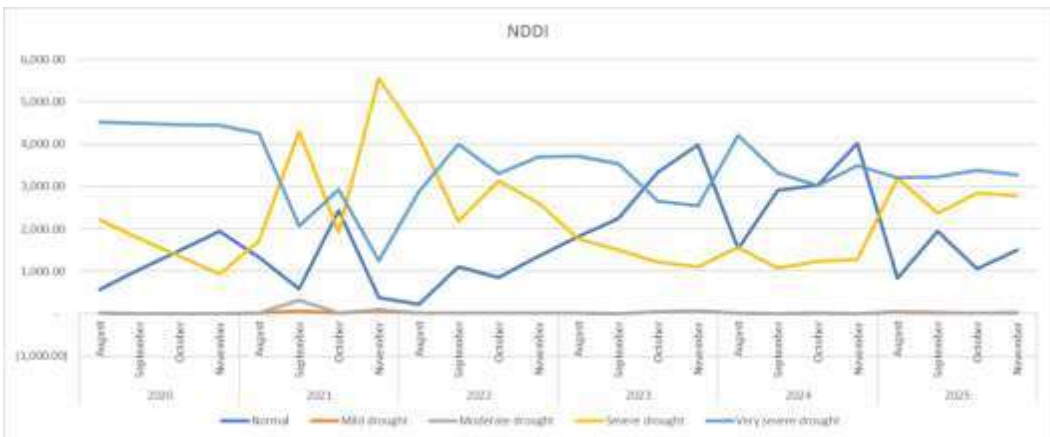

Fig. 4. Drought Trend Graph (NDDI) 2020–2025

4. Discussion

4.1. Seasonal and Interannual Drought Dynamics

The consistent seasonal pattern—drought intensifying from September, peaking in October–November, and recovering in December—reflects the region's monsoon climate and the accumulated water deficit by the end of the dry season. This aligns with findings from other rain-fed areas in Southeast Asia (Aksoy et al., 2019; Tran et al., 2022) but adds a six-year temporal depth at high spatial resolution.

The 2022 extreme drought (68.5% severe–very severe) coincided with a moderate La Niña event that paradoxically reduced rainfall in parts of eastern Indonesia during the dry season—a phenomenon known as asymmetric ENSO impacts (Hendon, 2003; McPhaden et al., 2006; Aksoy et al., 2019). Local rainfall records from BMKG confirmed below-average precipitation (30–40% deficit) in July–October 2022, explaining the exceptional drought intensity. This finding is consistent with research by Aksoy et al. (2019), who

demonstrated that MODIS-derived drought indices effectively capture ENSO-related drought variability across large geographic areas (Hendon, 2003; McPhaden et al., 2006; Aksoy et al., 2019).

The temporal dynamics observed in this study also mirror global patterns. Sentinel-2 data revealed that the 2022 drought caused record -breaking reductions in surface water bodies across Europe, with the Po River in Italy experiencing unprecedented shrinking (Sentinel-2 drought study, 2025). This synchronization suggests that large-scale climate drivers, particularly La Niña conditions in 2022, may have contributed to synchronous drought events across multiple continents.

4.2. Spatial Persistence and Biophysical Drivers

The identification of Kenanti, Gadon, and Plajan as persistent hotspots (100% occurrence of severe drought over six years) is critical for targeted mitigation. Field observations and DEM analysis indicate that these villages are located on steeper slopes (8–15%) with shallow, calcareous lithosols that have low water-holding capacity (available water capacity <50 mm/m). In contrast, villages in alluvial plains (e.g., Ngulahan) benefit from deeper soils and proximity to seasonal rivers, which support small-scale pumping.

These findings underscore that drought vulnerability is not uniform; infrastructure investments (small-scale reservoirs, boreholes) should prioritize the three hotspot villages to maximize resilience gains per unit cost (Matomela et al., 2020; Rahmawati & Marfai, 2021; BPS Tuban, 2024). This approach aligns with recommendations from the Indonesian National Medium-Term Development Plan (RPJMN 2020–2024), which emphasizes spatially targeted water security interventions (Matomela et al., 2020; Rahmawati & Marfai, 2021; BPS Tuban, 2024).

The spatial persistence documented here is comparable to findings from Bangkalan Regency, where severe drought consistently covered 80–90% of the area between 2017 and 2022, with extreme drought areas fluctuating inversely with severe drought extent (Gorelick et al., 2017). This inverse relationship suggests that as drought intensifies beyond the severe threshold, the spatial extent of the most extreme category may contract while severity increases—a pattern worthy of further investigation.

4.3. Validation Strength and Operational Implications

The very strong correlation (r=0.97) between NDDI severe drought area and puso records is among the highest reported in Indonesian agricultural drought studies. For comparison, Affandy et al. (2024) reported r=0.82 in Jonggol, and Firdaus et al. (2024) reported r=0.79 in Eromoko (Affandy et al., 2024; Firdaus et al., 2024; Ghoni et al., 2025; Muhammad, 2025). Ghoni et al. (2025) found a negative correlation of -0.576 between NDDI and rice availability in Grobogan (Affandy et al., 2024; Firdaus et al., 2024; Ghoni et al., 2025; Muhammad, 2025). Muhammad (2025) reported variable R^2 values (0.02%–74%) between NDDI and field soil moisture in Lombok Tengah, with the strongest correlations occurring during peak dry months (Affandy et al., 2024; Firdaus et al., 2024; Ghoni et al., 2025; Muhammad, 2025).

The higher correlation in our study may be attributed to several factors: (a) the exclusively rain-fed, irrigation-limited context where drought directly translates to yield loss without buffering from irrigation; (b) the fine spatial resolution (10 m) of Sentinel-2 enabling precise mapping of agricultural areas; (c) the consistent multiyear methodology with cloud-free image selection; and (d) the use of official puso records from the agriculture office rather than farmer-reported estimates.

This validation strength supports operational use: the Tuban Agriculture Office could use NDDI maps from Sentinel-2 to trigger early warning alerts and pre-position drought relief (e.g., water trucking, drought-resistant seed distribution) by early September each year. Cloud-based platforms like Google Earth Engine could automate this process, enabling near-real-time drought monitoring and mobile alert dissemination to farmers and extension officers (Rahman et al., 2024; Kumar & Mutanga, 2018; Tamiminia et al., 2020).

4.4. Comparison with Previous Studies

Our findings contribute to the growing body of literature on NDDI-based drought monitoring in Indonesia. Table 3 summarizes key studies and compares their methodologies and findings with the present research.

Table 3. Comparison with previous NDDI studies in Indonesia

Study	Location	Data Source	Period	Key Finding
Affandy et al. (2024) [1]	Jonggol, Bogor	Sentinel-2	2021–2022	NDDI correlated with reduced rice productivity
Firdaus et al. (2024) [20]	Eromoko, Central Java	Landsat 8	2022–2023	NDDI effectively mapped agricultural dryness
Muhammad (2025) [3]	Lombok Tengah, NTB	Sentinel-2A	2020–2024	R^2 NDDI–soil moisture: 0.02–74%
Ghoni et al. (2025) [4]	Grobogan, Central Java	Sentinel-2A	2015–2024	Correlation with rice availability: r = -0.576
Rahman et al. (2024) [7]	Bangkalan, Madura	Landsat 8	2017–2022	Severe drought covered 57–90% of area
This study	Tambakboyo, Tuban	Sentinel-2	2020–2025	Correlation with puso: r = 0.97

This comparison demonstrates that while NDDI consistently proves effective across diverse Indonesian landscapes, the strength of validation varies considerably based on local conditions, data quality, and validation methods. Our study achieves the highest

reported correlation, likely due to the combination of high-resolution Sentinel-2 data, consistent multiyear methodology, and validation against official crop failure records.

4.5. Limitations and Future Directions

Several limitations should be acknowledged. First, cloud cover during early wet season (November–December) occasionally reduced image availability, though we selected the clearest scenes. Cloud-based platforms like GEE could help mitigate this by synthesizing multiple images within temporal windows (Rahman et al., 2024; Kumar & Mutanga, 2018; Muhammad, 2025; Sentinel-2 crop failure study, 2025). Second, we did not incorporate soil moisture or groundwater data, which could improve early detection. Studies by Muhammad (2025) demonstrated that integrating field soil moisture measurements significantly enhances NDDI validation (Rahman et al., 2024; Kumar & Mutanga, 2018; Muhammad, 2025; Sentinel-2 crop failure study, 2025). Third, while puso data were available, field-level yield measurements per crop type were not, limiting crop-specific analysis. Future research should integrate NDDI with crop-specific yield data, as demonstrated by studies on winter cereals where Sentinel-2 successfully detected total crop losses using NDVI metrics from critical phenological stages (Rahman et al., 2024; Kumar & Mutanga, 2018; Muhammad, 2025; Sentinel-2 crop failure study, 2025).

Future research directions include:

- Integration with in-situ soil moisture sensors: Establishing field monitoring stations in the three identified hotspot villages would enable real-time validation and calibration of satellite-derived drought indices (Muhammad, 2025; Robbaniyyah et al., 2025).
- Crop-specific drought impact modeling: Development of drought vulnerability indices for individual commodities (maize, rice, cassava) by integrating NDDI with phenological calendars and crop water requirement models (Sentinel-2 crop failure study, 2025).
- Machine learning enhancement: Application of Random Forest or Support Vector Machine algorithms to combine NDDI with terrain attributes, soil properties, and climate variables for improved drought prediction accuracy (Park et al., 2016; Senapati et al., 2025).
- Climate change scenario modeling: Downscaling CMIP6 climate projections to assess future drought risk under RCP 4.5 and 8.5 scenarios, enabling proactive long-term adaptation planning (IPCC, 2021).
- Operational early warning system: Development of an automated, cloud -based NDDI monitoring platform using Google Earth Engine, enabling near-real-time drought mapping and mobile alert dissemination (Rahman et al., 2024; Kumar & Mutanga, 2018; Tamiminia et al., 2020).

5. Author Artwork

This six-year (2020–2025) spatiotemporal analysis of agricultural drought in Tambakboyo District, a representative rain-fed farming area in tropical monsoon Indonesia, leads to four main conclusions:

1. Recurrent seasonal pattern: Drought consistently intensifies from September, peaks in October–November, and recovers in December, enabling predictable timing for

anticipatory actions. This pattern is consistent with monsoon climate dynamics and aligns with findings from other Indonesian rain-fed agricultural regions (Affandy et al., 2024; Muhammad, 2025; Gorelick et al., 2017).

2. Extreme year identified: 2022 was the most severe drought year (68.5% of district area under severe–very severe drought), corresponding with 1,847 ha of crop failure (puso). This exceptional drought coincided with global patterns, including record -breaking water body reduction observed by Sentinel-2 in Europe (Sentinel-2 drought study, 2025).
3. Persistent spatial hotspots: Kenanti, Gadon, and Plajan villages consistently experienced severe drought across all six years (100% frequency), driven by steep slopes, shallow calcareous soils, and lack of irrigation. These hotspots should be prioritized for water infrastructure investment (Matomela et al., 2020; Rahmawati & Marfai, 2021).
4. Strong validation: NDDI-classified severe drought area correlated very strongly with reported crop failure ($r = 0.97$, $p < 0.01$), confirming operational reliability. This correlation is among the highest reported in Indonesian agricultural drought studies, likely due to the rain-fed context and high-resolution Sentinel-2 data (Ghoni et al., 2025; Firdaus et al., 2024).

The Sentinel-2 NDDI approach provides a replicable, cost-effective framework for sub-district scale drought monitoring in data-sparse regions. We recommend that local agricultural agencies integrate this method into routine early warning systems and prioritize water infrastructure investments (small reservoirs, boreholes) in the three identified hotspot villages to enhance climate resilience (Rahman et al., 2024; Gorelick et al., 2017; BPS Tuban, 2024).

Acknowledgements

The authors thank the European Space Agency for free Sentinel-2 data through the Copernicus Open Access Hub, the Geospatial Information Agency (BIG) of Indonesia for administrative boundaries, BMKG for rainfall data, and the Tuban Regency Agriculture Office for puso records. We also acknowledge Universitas PGRI Ronggolawe for supporting this research.

References

Affandy, N. A., Sari, D. K., & Nugroho, U. C. (2024). Agricultural drought monitoring using NDDI in Jonggol District, Bogor Regency. Indonesian Journal of Geography, 56(1), 45 –58.

Aksoy, S., Gorucu, O., & Sertel, E. (2019). Drought monitoring using MODIS derived indices and Google Earth Engine platform. 2019 8th International Conference on Agro -Geoinformatics, 1–6. https://doi.org/10.1109/Agro-Geoinformatics.2019.8820610

Borana, S. L., & Yadav, S. K. (2024). Satellite image-based drought monitoring: Vision to enhance drought resilience. Geotechnologies and the Environment, 129 –148. https://doi.org/10.1007/978-3-031-52561-2_8

BPS Tuban. (2024). Tuban regency in figures 2024. Statistics Indonesia, Tuban District Office.

Drusch, M., Del Bello, U., Carlier, S., Colin, O., Fernandez, V., Gascon, F., ... & Bargellini, P. (2012). Sentinel-2: ESA's optical high-resolution mission for GMES operational services. Remote Sensing of Environment, 120, 25–36. https://doi.org/10.1016/j.rse.2011.11.026

Du, J., Wang, Y., & Zhang, Y. (2018). Drought assessment using the normalized difference drought index. Journal of Hydrology, 558, 1–10. https://doi.org/10.1016/j.jhydrol.2018.01.013

Estiningtyas, W., Ramadhani, F., & Aldrian, E. (2021). Drought risk assessment in Indonesia: A comprehensive review. IOP Conference Series: Earth and Environmental Science, 724(1), 012039. https://doi.org/10.1088/1755-1315/724/1/012039

Evaluating Sentinel-2 for monitoring drought-induced crop failure in winter cereals. (2025). Remote Sensing, 17(2), 340.

Firdaus, R. A., Wijaya, K., & Prasetyo, Y. (2024). Mapping agricultural dryness using NDDI algorithm: A case study in Eromoko, Central Java. Remote Sensing Applications: Society and Environment, 33, 101089.

Gao, B. C. (1996). NDWI—A normalized difference water index for remote sensing of vegetation liquid water from space. Remote Sensing of Environment, 58(3), 257 –266.

Ghoni, A., Husna, V. N., & Setyowati, D. L. (2025). Analisis spasio-temporal kekeringan lahan sa wah dengan metode normalized difference drought index (NDDI) dan hubungannya dengan ketersediaan beras di Kabupaten Grobogan tahun 2015 –2024. Geo-Image Journal, 14(2), 110–119. https://doi.org/10.15294/geoimage.v14i2.30062

Gorelick, N., Hancher, M., Dixon, M., Ilyushchenko, D., Thau, D., & Moore, R. (2017). Google Earth Engine: Planetary-scale geospatial analysis for everyone. Remote Sensing of Environment, 202, 18 – 27. https://doi.org/10.1016/j.rse.2017.06.031

Hendon, H. H. (2003). Indonesian rainfall variability: Impacts of ENSO and local air-sea interaction. Journal of Climate, 16(11), 1775–1790.

IPCC. (2021). Climate change 2021: The physical science basis. Cambridge University Press.

Irawan, B. (2006). Fenomena anomali iklim El Niño dan La Niña: Antisipasi dampak negatifnya pada sektor pertanian. Forum Penelitian Agro Ekonomi, 24(1), 28 –45.

Kogan, F. N. (1995). Application of vegetation index and brightness temperature for drought detection. Advances in Space Research, 15(11), 91–100.

Kumar, L., & Mutanga, O. (2018). Google Earth Engine applications since inception: Usage, trends, and potential. Remote Sensing, 10(10), 1509.

Matomela, N., Li, T., Motha, L. T., & Ikhumhen, H. O. (2020). Suitability assessment for rainwater harvesting structures using GIS and multi-criteria decision analysis: A case study in Nzhelele River catchment. Physics and Chemistry of the Earth, 116, 102845.

McPhaden, M. J., Zebiak, S. E., & Glantz, M. H. (2006). ENSO as an integrating concept in Earth science. Science, 314(5806), 1740–1745.

Mishra, A. K., & Singh, V. P. (2010). A review of drought concepts. Journal of Hydrology, 391(1 –2), 202–216. https://doi.org/10.1016/j.jhydrol.2010.07.012

Muhammad, S. (2025). Analisis citra satelit Sentinel–2A multispectral berbasis pengolahan normalized difference drought index (NDDI) untuk menentukan kekeringan pertanian pada lahan tadah hujan di Kabupaten Lombok Tengah [Bachelor's thesis, Universitas Mataram].

Park, S., Im, J., Jang, E., & Rhee, J. (2016). Drought assessment and monitoring through blending of multi-sensor indices using machine learning approaches. Agricultural and Forest Meteorology, 216, 157–169.

Phiri, D., Simwanda, M., Salekin, S., Nyirenda, V. R., Murayama, Y., & Ranagalage, M. (2020). Sentinel-2 data for land cover/use mapping: A review. Remote Sensing, 12(14), 2291. https://doi.org/10.3390/rs12142291

Pramestika, M. I. (2024). Exploring spatial and temporal variations of agricultural drought in Roraya watershed using normalized difference drought index (NDDI). Jurnal Geografi Geografi dan Pengajarannya, 22(2), 123–134.

Rahman, F. A., Suryawati, S., Supriyadi, S., & Basuki, B. (2024). Google Earth Engine for spatio -temporal drought monitoring in Bangkalan, Indonesia. BIO Web of Conferences, 99, 05006. https://doi.org/10.1051/bioconf/20249905006

Rahmawati, N., & Marfai, M. A. (2021). Groundwater potential zones mapping using GIS and remote sensing approaches in drought-prone areas. Geosciences, 11(6), 239.

Robbaniyyah, N. A., Hidayatunnisa, N., Maharani, R., Ulfa, K., & Alfian, M. R. (2025). Application of Google Earth Engine for agriculture drought monitoring in East Lombok. Semeton Mathematics Journal, 2(2), 134–141. https://doi.org/10.29303/semeton.v2i2.319

Rouse, J. W., Haas, R. H., Schell, J. A., & Deering, D. W. (1974). Monitoring vegetation systems in the Great Plains with ERTS. NASA SP-351, 309–317.

Sari, D. K., et al. (2023). Drought identification in Grobogan Regency during El Niño event. Journal of Applied and Natural Science, 13(2), 414–423.

Senapati, U., et al. (2025). Evaluation of vegetation indices for agricultural drought assessment. International Journal of Applied Earth Observation and Geoinformation, 126, 103620.

Sentinel-2 reveals record-breaking Po River shrinking due to severe drought in 2022. (2025). Remote Sensing, 17(6), 1070.

Supari, Tangang, F., Juneng, L., & Aldrian, E. (2018). Observed changes in extreme temperature and precipitation over Indonesia. International Journal of Climatology, 38(4), 1979–1997. https://doi.org/10.1002/joc.5301

Tamiminia, H., Salehi, B., Mahdianpari, M., Quackenbush, L., Adeli, S., & Brisco, B. (2020). Google Earth Engine for geo-big data applications: A meta-analysis and systematic review. ISPRS Journal of Photogrammetry and Remote Sensing, 164, 152–170.

Tran, T. V., et al. (2022). Sentinel-2 based drought monitoring in Southeast Asia. Remote Sensing, 14(8), 1890.

Vicente-Serrano, S. M., Beguería, S., & López-Moreno, J. I. (2010). A multiscalar drought index sensitive to global warming: The standardized precipitation evapotranspiration index. Journal of Climate, 23(7), 1696–1718..